# Predictive control of a nonlinear distributed parameter system: Real time control of a painting film drying process

Mohamed-Chaker Larabi, Pascal Dufour, Pierre Laurent, Youssoufi Touré

1
Université de Lyon, Lyon, F-69003, France; Université Lyon 1;
CNRS UMR 5007 LAGEP (Laboratoire d'Automatique et de GEnie des Procédés),
43 bd du 11 novembre, 69100 Villeurbanne, France
Tel +33 (0) 4 72 43 18 45 - Fax +33 (0) 4 72 43 16 99
http://www-lagep.univ-lyon1.fr/ http://www.univ-lyon1.fr http://www.cnrs.fr

2
Université d'Orléans,
UPRES EA 2078 LVR (Laboratoire de Vision et de Robotique ),
63 Av de Lattre de Tassigny, 18020 Bourges Cedex, France
http://www.bourges.univ-orleans.fr/rech/lvr/

# Predictive control of a nonlinear distributed parameter system : real time control of a painting film drying process

M.C. Larabi[1], P. Dufour [1*], P. Laurent[1], Y. Touré[2]
[1] LAGEP UPRES-A CNRS Q 5007
University Claude Bernard Lyon 1
43, bd du 11 Novembre 1918
69622 Villeurbanne Cedex, France
{larabi,dufour,laurent}@lagep.univ-lyon1.fr
[2] LVR UPRES EA 2078
University of Orléans
63, avenue de Lattre de Tassigny
18020 Bourges Cedex, France
Youssoufi.Toure@bourges.univ-orleans.fr

**Keywords:** Nonlinear distributed parameter system, predictive control, constraints handling, drying process, real time control.

## Abstract

This paper deals with the model predictive control of processes. The new step is the use of a distributed parameter system instead of a lumped parameter system. The internal model control structure is also used to solve the trajectory tracking problem. The internal model is obtained from the linearization of the initial set of nonlinear partial differential equations about the desired trajectory. Finally, the control problem stated as a constrained optimization problem is solved by a control algorithm. Experimental results presented here show the efficiency of this control strategy.

## 1 Introduction

This work is concerned with a model based approach to the nonlinear parabolic distributed parameter system control. There are few practical works directly dealing with the control of such systems. Even if the existed one are based on interesting structures, they treat neither complex nonlinearities nor a set of partial differential equations [6, 5]. Besides, these results do not seem to be applicable to nonlinear models like the described one in this paper.
The control synthesis is reached by extending the classical use of the model predictive control (MPC) strategy [9, 11, 10] from systems described by ordinary differential equations to systems described by partial differential equations. This leads to a control problem stated as a constrained optimization problem. Moreover this strategy is combined here with the internal model control structure (IMC) [8] where the model is obtained by the off-line linearization of the initial nonlinear model about a given trajectory. This allows to decrease the on-line calculation time due to the model resolution needed in the constrained optimization problem resolution. Indeed, this is an important problem to be kept in mind for real time control.
In the first section, we present the drying plant described by a nonlinear distributed parameter system . The control problem is then exposed. In the next section, MPC strategy and the resolution method are explained in more details. Experimental results are finally exposed to show the possibilities for this approach in real time control applications.

* Author to whom all correspondence should be addressed.

## 2 Drying process and control problem

### 2.1 Drying process

Within the framework of a previous study [1], an experimental drying process has been built. It allows to dry a painting film sample coated on a car iron support by supply of an infrared flow. The plant is represented Fig. 1 with the infrared part and with the instrumention part. The sensors are : a pyrometer that allows the on-line temperature measurement of the sample at the upper surface and a precision balance that allows the follow-up of the sample and support set mass. The painting film sample mass is the sum of the constant final dried mass of the sample with the time variant water mass in the sample. Indeed, during the drying under infrared flow, this water mass decreases since the water contained in the painting film sample migrates from inside to the upper surface and vaporizes at this surface.

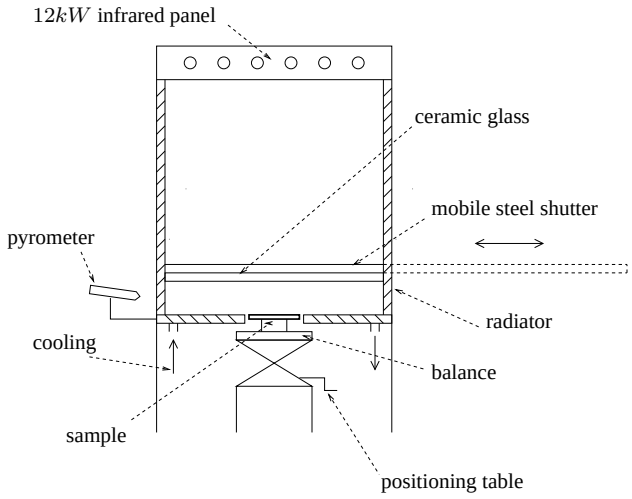


Figure 1: Drying process.

These mass and temperature measurements during experimental drying kinetics have allowed to validate the knowledge model that we use in this paper : this low thickness painting film sample is characterised by its temperature assumed uniform $T(t)$ and by its dry basis humidity $\chi(z,t)$ assumed to varying only according to the thickness $z$ of the sample [1].
The drying leads to water losses which produces a variation in the sample geometry. Considering the surface size and the thickness of the sample, we consider that the water extraction leads only to the linear reduction of the sample thickness $e_p$ with respect to the mean humidity $\bar{\chi}$ :

$$e_p = e_{sec}(1 + \phi\bar{\chi}) \tag{1}$$

where $e_{sec}$ is the final dried thickness of the sample and with :

$$\bar{\chi}(t) = \frac{1}{e_{sec}} \int_0^{e_{sec}} \chi(z,t)\, dz \tag{2}$$

The model of the painting film sample infrared drying can be finally represented by the state variables $T(t)$ and $\chi(z,t)$. It is deduced from the following energical and mass balances (remaining expressions are given in the annexe).

### 2.2 Energical balance

We assume that the car iron support is a reliable enough thermical conductor to consider that the temperature $T$ is uniform on the sample and support set. Taking into account of the different losses $P_i$ as well as the absorbed infrared flow represented Fig. 2,

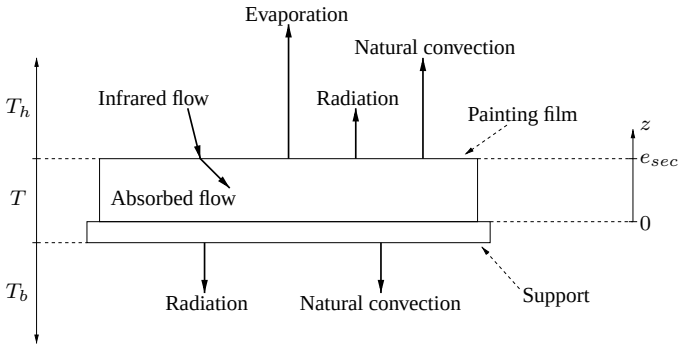


Figure 2: Thermal flows.

the energical balance leads to :

$$(\rho_p C_p(\bar{\chi},T)e_p + \rho_s C_s e_s)\frac{dT}{dt} = -\sum_{i=1}^{5} P_i + P_{abs} \tag{3}$$

where $\rho_p C_p(\bar{\chi},T)e_p$ and $\rho_s C_s e_s$ are respectively the surface thermal capacity of the painting film sample and the surface thermal capacity of the support.
Different losses due to the natural convection and radiation phenomena on both surfaces have for expression :

$$P_1 = h_c(T - T_h) \tag{4}$$
$$P_2 = \sigma_h(T^4 - T_h^4) \tag{5}$$
$$P_3 = h_c(T - T_b) \tag{6}$$
$$P_4 = \alpha_s\, \sigma(T^4 - T_b^4) \tag{7}$$

The water loss $P_5$ is linked to the drying velocity $\dot{m}(\bar{\chi},T)$ :

$$P_5 = l_v(T)\dot{m}(\bar{\chi},T) \tag{8}$$

and the absorbed flow $P_{abs}$ depends on the manipulated variable, i.e. the infrared flow $\varphi_{ir}(t)$ :

$$P_{abs} = \alpha_{ir}(\bar{\chi})\varphi_{ir} \tag{9}$$

### 2.3 Mass balance

Since there is no macroporous structure, we consider that the water migrates only by diffusion phenomenon. It allows to write the mass balance using the Fick law :

- for $z \in \Omega = ]0, e_{sec}[$ :

$$\frac{\partial\chi}{\partial t} = \frac{\partial}{\partial z}[D_{eff}(\chi,T)\frac{\partial\chi}{\partial z}] \tag{10}$$

with the effective diffusion coefficient $D_{eff}$ depending on the humidity and the temperature :

$$D_{eff}(\chi,T) = \frac{D_0 exp^{(\frac{-a}{\chi})} exp^{(\frac{-Ea}{RT})}}{(1+\phi\chi)^2} \tag{11}$$

- at $z = 0$, i.e. at the painting film sample lower surface, there is not any mater transfert :

$$\frac{\partial \chi}{\partial z} = 0 \tag{12}$$

- at $z = e_{sec}$, the outgoing flow is linked to the drying velocity through :

$$-D_{eff}(\chi, T)\frac{\partial \chi}{\partial z} = \frac{\dot{m}(\bar{\chi}, T)}{\rho} \tag{13}$$

### 2.4 Nonlinear distributed parameter system

From the previous energical and mass balances, the process is represented by the following nonlinear distributed parameter system $(\mathcal{S}_{NL})$ :

$$(\mathcal{S}_{NL}) \begin{cases} \frac{\partial \chi}{\partial t} = F_1(\frac{\partial^2 \chi}{\partial z^2},\ \frac{\partial \chi}{\partial z},\ \chi,\ T) \text{ for } z \in \Omega,\ t > 0 \\ \frac{dT}{dt} = F_2(\bar{\chi},\ T) + F_3(\bar{\chi}, T)u(t) \text{ for } t > 0 \\ \text{with :} \\ \text{the scalar input : } u(t) = \varphi_{ir}(t) \text{ for } t > 0 \\ \text{the output : } y_m(t) = T(t) \text{ for } t > 0 \\ \text{with the boundary conditions :} \\ \frac{\partial \chi}{\partial z} = 0 \text{ for } z = 0,\ t > 0 \\ F_4(\frac{\partial \chi}{\partial z}, \bar{\chi}, \chi, T) = 0 \text{ for } z = e_{sec},\ t > 0 \\ \text{with the initial conditions :} \\ \chi(z, 0) = \chi_i \text{ for } z \in \Omega \cup \{0,\ e_{sec}\} \\ T(0) = T_i \end{cases} \tag{14}$$

**Remark 2.1** *According to the spatial uniform property assumption on the temperature, the control problem is a distributed control one : indeed the manipulated variable, i.e. the infrared flow $\varphi_{ir}(t)$, acts instantaneously at the boundary $(z = e_{sec})$ and over the painting film sample.*

### 2.5 Control problem statement

For real applications, the final product obtained by the painting film sample drying has to be usable : bubbles and fissures phenomena have therefore to be avoided. To ensure the final product quality, paint producers propose a reference temperature profile during the drying cycle (temperature rising with a constant velocity and upholding at a given temperature).
The control problem considered here is the tracking of the temperature reference trajectory shown Fig. 3, subject to constraints on the manipulated variable $u(t)$.

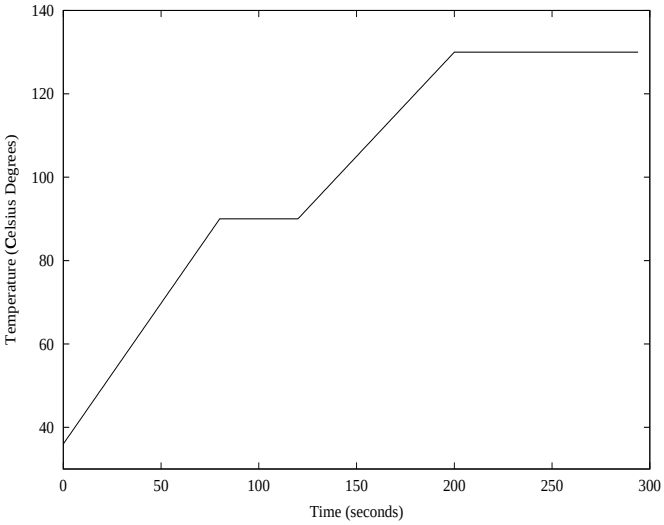


Figure 3: Temperature reference trajectory.

**Remark 2.2** *This reference could be the result of an off-line optimization problem like in [3]. The ideal optimal problem would consist in finding the way to simultaneously achieve the drying as far as possible and to handle the bubbles and fissures phenomena. A modeling for such problems is unfortunately not available yet.*

Considering this constrained control problem, a MPC strategy seems to be well-adapted to satisfy such control requirements.

## 3 Predictive control strategy

### 3.1 Constrained optimization problem

A reference trajectory tracking problem can be achieved by the use of the internal model control structure (IMC) [8] depicted Fig. 4 where the manipulated variable is applied to both process and model.

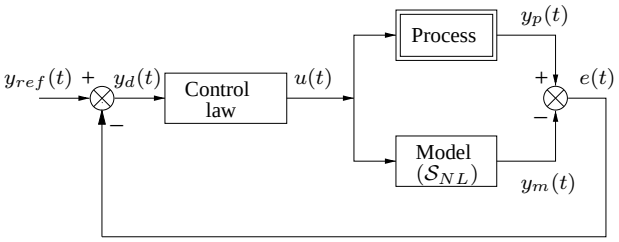


Figure 4: IMC principle.

The objective is to determine a control law such that the process output $y_p(t)$ tracks some reference $y_{ref}(t)$ in spite of some modeling errors. This control strategy can be an explicit control law for linear time invariant systems even for distributed parameter system [12]. But for nonlinear or time

variant system, a more feasible approach is the indirect one. In a previous work [2], we introduce a MPC strategy to deal with the trajectory tracking task. The mathematical discrete-time formulation, for a SISO process, can be written as the following constrained optimization problem :

$$\begin{cases} \min\limits_{\tilde{u}} J(\tilde{u}) = \sum\limits_{j=k+1}^{j=k+N_p} [y_{ref}(j) - y_p(j)]^2 \\ \tilde{u} = [\varphi_{ir}(k) \; ... \; \varphi_{ir}(k+N_c-1)]^T \\ \text{and } \forall j \in \mathcal{J} = \{k+N_c, \; ..., \; k+N_p-1\} : \\ u(j) = u(k+N_c-1) \\ \text{subject to constraints on the manipulated variable.} \end{cases} \tag{15}$$

First of all, the knowledge of $y_p(j)$ over the prediction horizon $N_p$ is not available at the present time $k$. Due to the IMC, this problem can be solved by reformulating the tracking problem :

$$y_{ref}(j) - y_p(j) = y_d(j) - y_m(j) \tag{16}$$
$$y_d(j) = y_{ref}(j) - e(j) \tag{17}$$

**Assumption 1** *The error $e(j)$ between the process output and the model output remains the same at each sample time $k$ over the prediction horizon $N_p$ [7, 8]. The error value is updated at each sampled time $k$.*

Then, according to (16) and assumption (1) the initial criterion $J$ to be minimized can be expressed as :

$$J(\tilde{u}) = \sum_{j=k+1}^{j=k+N_p} [y_d(j) - y_m(j)]^2 \tag{18}$$

From a practical point of view, the second problem is the computational time aspect. Indeed, in the MPC strategy, the model aims to predict the future dynamic behaviour of the process output over a finite prediction horizon $N_p$. To reduce the on-line model resolution time, we use a linearization method of the nonlinear model $(\mathcal{S}_{NL})$ about a similar nonlinear model $(S_0)$ computed off-line by choosing its input $u_0$. Then, a time variant linearized model $(S_{TVL})$ can represent the small state variations $\Delta\chi(k)$ $\Delta T(k)$ and small output variation $\Delta y_m(k)$ about $(S_0)$ with respect to small input variation $\Delta u(k)$ (Fig. 13 given in annexe).

$$u(k) = u_0(k) + \Delta u(k) = \varphi_{ir0}(k) + \Delta\varphi_{ir}(k) \tag{19}$$
$$\chi(k) = \chi_0(k) + \Delta\chi(k) \tag{20}$$
$$T(k) = T_0(k) + \Delta T(k) \tag{21}$$
$$y_m(k) = y_0(k) + \Delta y_m(k) \tag{22}$$

Finally, the off-line solved nonlinear model $(S_0)$ and the on-line solved linearized model $(S_{TVL})$ replace the initial nonlinear model $(\mathcal{S}_{NL})$ in the IMC structure (Fig 5).

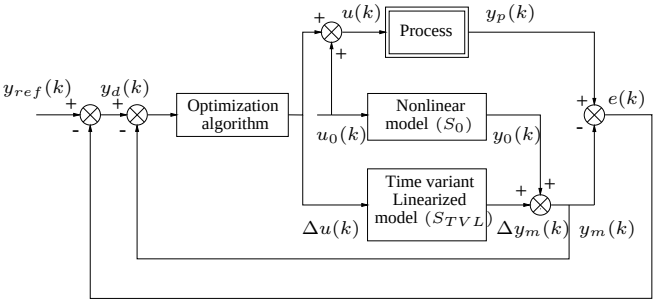


Figure 5: Time Variant Linearized Internal Model Control (TVLIMC) structure.

The objective is now to find the variation $\Delta u(k)$ of the manipulated variable $u(k)$ about a chosen trajectory $u_0(k)$ leading to the best optimization result. According to the TVLIMC structure, the trajectory tracking is now equivalent to the following constrained optimization problem :

$$\begin{cases} \min\limits_{\Delta\tilde{u}} J(\Delta\tilde{u}) = \sum\limits_{j=k+1}^{j=k+N_p} [y_d(j) - (y_0(j) + \Delta y_m(j))]^2 \\ \Delta\tilde{u} = [\Delta\varphi_{ir}(k) \; ... \; \Delta\varphi_{ir}(k+N_c-1)]^T \\ \Delta u(j) = \Delta u(k+N_c-1) \; \forall j \in \mathcal{J} \\ \text{subject to the time-variant linearized model } (\mathcal{S}_{LTV}) \; : \\ \quad \begin{cases} \frac{\partial \Delta\chi}{\partial t} = A_1(t)(\Delta X \; \Delta T)^T \text{ for } z \in \Omega, t \in T = ]kT_e, (k+N_p)T_e] \\ \frac{\partial \Delta T}{\partial t} = A_2(t)(\Delta X \; \Delta T)^T + A_3(t)\Delta u(t) \text{ for } t \in T \\ \text{with :} \\ \text{the scalar input : } \Delta u(t) = \Delta\varphi_{ir}(t) \text{ for } t \in T \\ \text{the output : } \Delta y_m(t) = \Delta T(t) \text{ for } t \in T \\ \text{with the boundary conditions :} \\ \frac{\partial \Delta\chi}{\partial z} = 0 \text{ for } z = 0, \; t \in T \\ A_4(t)(\Delta\chi \; \Delta T)^T = 0 \text{ for } z = e_{sec}, \; t \in T \\ \text{with the initial conditions :} \\ \Delta\chi(z,0) = 0 \text{ for } z \in \Omega \cup \{0, \; e_{sec}\} \\ \Delta T(0) = 0 \end{cases} \\ \text{and subject to constraints on the manipulated variables } \Delta\tilde{u} \end{cases}$$

where the time-variant linear operators $A_1(t)$, $A_2(t)$, $A_3(t)$ and $A_4(t)$ are deduced from the model linearization about $(\mathcal{S}_0)$ [2].

### 3.2 Constraints handling

The problem is now to find a method to handle magnitude and velocity constraints on the manipulated variable that follow into account ($T_e$ is the sampling period) :

$$u_{min} \leq u(j) \leq u_{max} \quad (24)$$

$$\Delta u_{min} \leq \frac{u(j)-u(j-1)}{T_e} \leq \Delta u_{max} \quad (25)$$

Since the manipulated variable is the only constrained variable, an easy method is the use of the following transformation method depicted Fig. 6.

$$\begin{cases} u(j) = f(p(j)) = f_{moy} + f_{amp} yanh[\frac{p(j)-f_{moy}}{f_{amp}}] \\ p(j) \in \mathbb{R}^{N_c} \end{cases} \quad (26)$$

with the following datas updated at each time $k$ :

$$\begin{cases} f_{moy} = \frac{f_{max}+f_{min}}{2} \\ f_{amp} = \frac{f_{max}-f_{min}}{2} \\ f_{min} = max[u_{min}, u(j-1) + \Delta u_{min} T_e] \\ f_{max} = min[u_{max}, u(j-1) + \Delta u_{max} T_e] \end{cases} \quad (27)$$

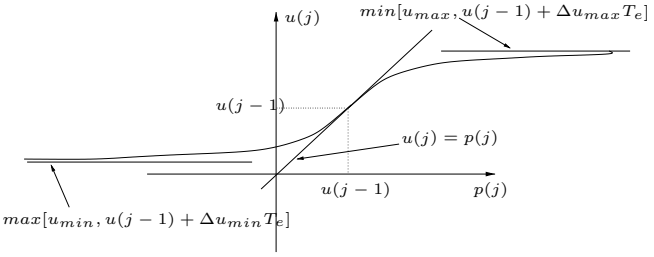


Figure 6: Transformation law.

Seeking now these unconstrained parameters $p(j)$ always ensures the constraints check on the manipulated variable.
Besides, from the linearization method and the function $f$ bijectivity we can also define the small variations of the new seeked parameter $p(j)$ about $p_0(j) = f^{-1}(u_0(j))$ :

$$\Delta p(j) = p(j) - p_0(j) \quad (28)$$

Finally, combining the constrained optimization problem $(23)$, the transformation law $f$ and the linearization method, we can define the final unconstrained optimization problem :

$$\begin{cases} \min\limits_{\Delta\tilde{p}} J(\Delta\tilde{p}) = \sum\limits_{j=k+1}^{j=k+N_p} [y_d(j) - (y_0(j) + \Delta y_m(j))]^2 \\ \Delta\tilde{p} = [f^{-1}(\Delta\varphi_{ir}(k)) \; ... \; f^{-1}(\Delta\varphi_{ir}(k+N_c-1))]^T \\ \Delta p(j) = f^{-1}(\Delta\varphi_{ir}(k+N_c-1)) \; \forall j \in \mathcal{J} \\ \Delta\tilde{p} \in \mathbb{R}^{N_c} \\ \text{subject to the time-variant linearized model } (\mathcal{S}_{LTV}) \; : \\ \begin{cases} \frac{\partial \Delta\chi}{\partial t} = A_1(t)(\Delta X \; \Delta T)^T \text{ for } z \in \Omega, \; t \in T \\ \frac{\partial \Delta T}{\partial t} = A_2(t)(\Delta X \; \Delta T)^T + A_3(t)\Delta u(t) \text{ for } t \in T \\ \text{with :} \\ \text{the scalar input : } \Delta u(t) = \Delta\varphi_{ir}(t) \text{ for } t \in T \\ \text{the output : } \Delta y_m(t) = \Delta T(t) \text{ for } t \in T \\ \text{with the boundary conditions :} \\ \frac{\partial \Delta\chi}{\partial z} = 0 \text{ for } z = 0, \; t \in T \\ A_4(t)(\Delta\chi \; \Delta T)^T = 0 \text{ for } z = e_{sec}, \; t \in T \\ \text{with the initial conditions :} \\ \Delta\chi(z,0) = 0 \text{ for } z \in \Omega \cup \{0, \; e_{sec}\} \\ \Delta T(0) = 0 \end{cases} \end{cases} \quad (29)$$

with the time variant linearized model input in the TVLIMC structure :

$$\Delta u(k) = u(k) - u_0(k) = f(p_0(k) + \Delta p(k)) - f(p_0(k)) \quad (30)$$

This unconstrained optimization problem $(29)$ can now be solved by any unconstrained optimization algorithm.

### 3.3 Resolution method

Widely known for its robustness and convergence properties, we apply the Levenberg-Marquardt's algorithm[4], where the variables $\Delta\tilde{p}$ are determined at each sample instant $k$ by the iteration procedure :

$$\Delta\tilde{p}^{i+1} = \Delta\tilde{p}^i - (\bigtriangledown^2 J^i_{tot} + \lambda I)^{-1} \; \bigtriangledown J^i_{tot} \quad (31)$$

where $\bigtriangledown J^i_{tot}$ and $\bigtriangledown^2 J^i_{tot}$ are the criteria gradient and the criteria hessian with respect to $\Delta\tilde{p}^i$.
This resolution algorithm is now implemented on the process and allows to track any kind of reference trajectory.

## 4 Experimental results

Experiments have been realized to point out the prediction horizon influence. In this first attempts, the unity control horizon is chosen.

### 4.1 Operating conditions

The operating conditions are the following one :

- the linearization about $(\mathcal{S}_0)$ is performed with $u_0 = 5000\ W.m^{-2}$ and with the initial conditions $T_i = 36\ ^oC$ and $\chi_i = 0.4\ kg.kg^{-1}$ ;
- the models $(\mathcal{S}_0)$ and $(S_{TVL})$ are solved by the finite volumes method (6 volumes) ;
- the sampling period $T_e$ value is 1 second ;
- constraints boundaries are :

$$u_{max} = 12,000\ W.m^{-2} \quad (32)$$
$$u_{min} = 0\ W.m^{-2} \quad (33)$$
$$\Delta u_{max} = +500\ W.m^{-2}.s^{-1} \quad (34)$$
$$\Delta u_{min} = -500\ W.m^{-2}.s^{-1} \quad (35)$$

- atmospheric conditions are :

$$\chi_{air} = 20\% \quad (36)$$
$$T_h = 52\ ^oC \quad (37)$$
$$T_b = 20\ ^oC \quad (38)$$

- the control algorithm, written in Fortran code, has been combined to C code in order to realize the interface with the sensors and the actuator ;
- the processor rate is $400MHz$.

### 4.2 Temperature reference trajectory tracking

From Fig. 7 and Fig. 8, we can see that the tracking objective is correctly achieved.
Moreover, the intermediate value $6s$ for the horizon prediction gives the best result. It can notably be explained by the discontinuities handling (at $k = 80s$, $120s$ and $200s$) for each horizon prediction value :

- with a small prediction horizon $(N_p = 3s)$, the discontinuities handling is less efficient than with $N_p = 6s$ as we can see for the values taken by the criteria $J$ (Fig 9). In this case, informations quantity available describing the future process behaviour are insufficient. In a way, with $N_p = 3s$ the problem is badly stated for its resolution, as we can see on the applied control : when the three discontinuities points appear, the infrared flow is always either satured on its magnitude (Fig. 10) or on its velocity (Fig. 11). This means that the algorithm tends too often to find a non admissible solution. This leads consequently to poor tracking performances ;

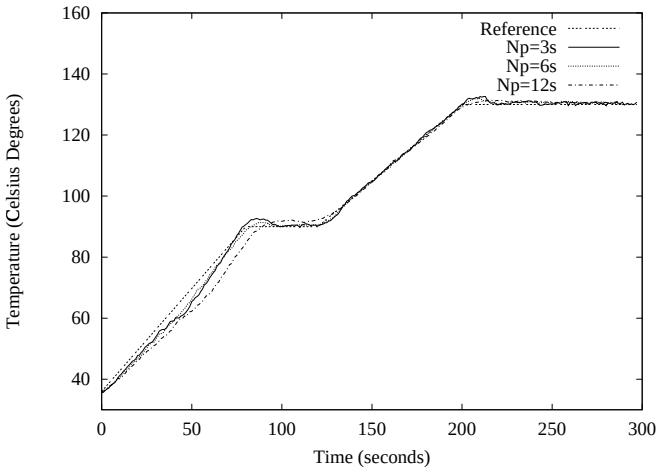


Figure 7: Reference tracking for $N_p = 3s,\ 6s,\ 12s$.

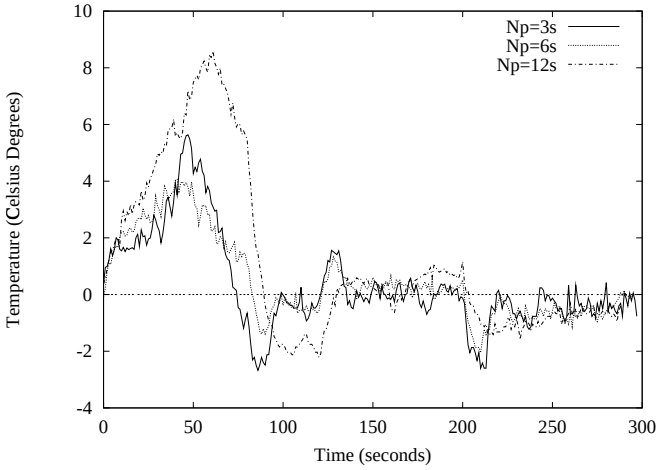


Figure 8: Tracking error for $N_p = 3s,\ 6s,\ 12s$.

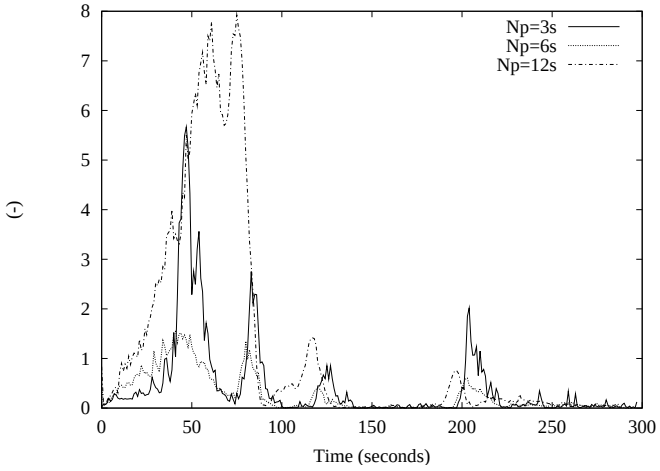


Figure 9: Criteria values sequence for $N_p = 3s,\ 6s,\ 12s$.

- increasing the prediction horizon value to $6s$ and $12s$, the infrared flow becomes more and more smooth

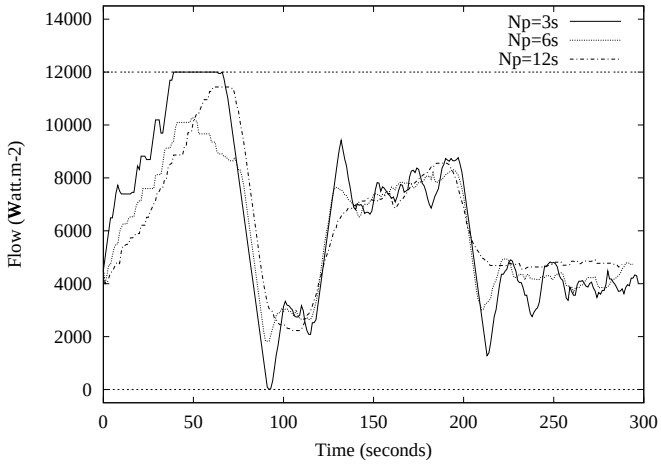


Figure 10: Control magnitude for $N_p = 3s,\ 6s,\ 12s$.

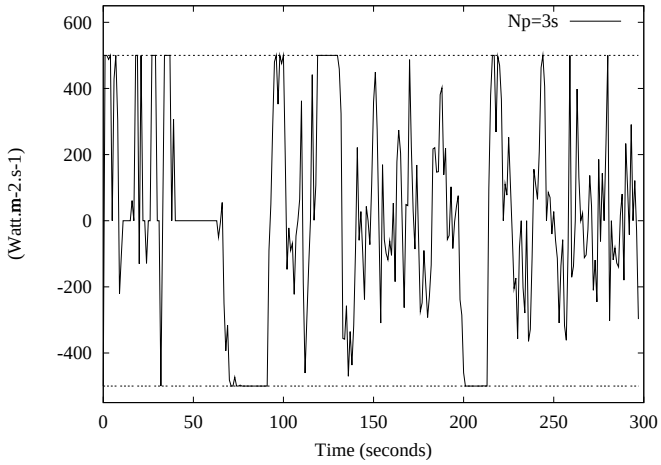


Figure 11: Control velocity for $N_p = 3s$.

(Fig. 10), but with a big prediction horizon $(N_p = 12s)$, another problem appears : the model, qualitatively true, is quantitatively false (Fig. 12). Since more values calculated by the model resolution are taken into account in the optimization problem, the criteria minimization is less efficient than in the case where the prediction horizon take an average value for $(N_p = 6s)$ (Fig 9).

Therefore, the prediction horizon value $N_p = 6s$ is the "optimal" choice for this main parameter.
Moreover, one of the property of the IMC structure is confirmed by these experimental results : the tracking is effective in spite of the model output used to find the control algorithm does not track quantitatively the temperature reference trajectory (Fig. 12).

## 5 Conclusion

In this paper, we have developed an efficient approach for an on-line control problem. It dealed with the trajectory tracking problem of the process output. We have presented a control strategy combining both the model based predictive control and the internal model control structure. The new advance in the MPC strategy is the use of a distributed parameter system instead of a lumped parameter system. Since the on-line control algorithm seeks the manipulated variable by solving the model, we also use an off-line linearization method.
Experimentals results have shown the efficiency of the MPC strategy : the influence of the prediction horizon has been shown. A trade off has to be found between smallest value that leads to a badly stated optimization problem and a long horizon control. In this latter case, since too many quantitatively false model informations are computed during the final unconstrained optimization problem resolution, the final control does not lead to good tracking performances.
In perspective, others results concerning the application of this predictive control strategy to another nonlinear distributed parameter system with output constraints handling will be published. It deals with the destruction of volatile organic compounds (VOC) by catalytic reaction.
As for the theoretical perspectives, the accurate characterisation and the closed loop stability study are expected.

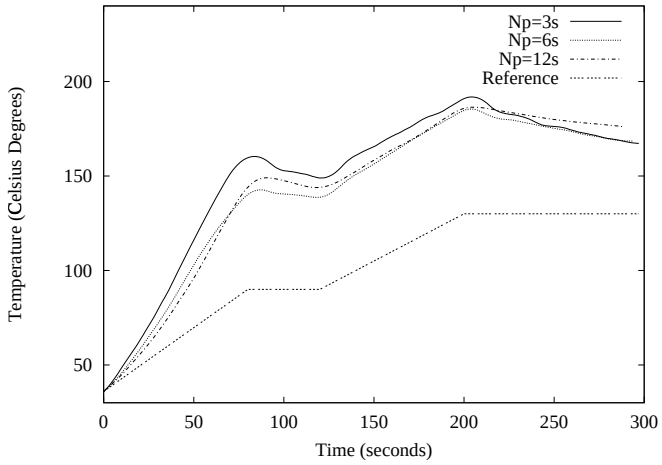


Figure 12: Model output for $N_p = 3s,\ 6s,\ 12s$.

## 6 Annexe

### 6.1 Scheme

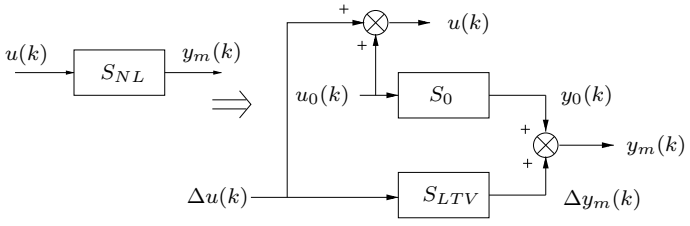


Figure 13: Model linearization.

### 6.2 Drying velocity

The pressure difference between the sample and the ambiant air leads to an inside out water migration. This is characterised by the drying velocity $\dot{m}(\bar{\chi}, T)$ :

$$\dot{m}(\bar{\chi}, T) = \frac{k_m m_v}{R} P_t \frac{2}{T + T_h} log_{10}[\frac{P_t - \chi_{air} P_{v_{sat}}(T_h)}{P_t - a_w(\bar{\chi}) P_{v_{sat}}(T)}] \quad (39)$$

where the saturated vapor saturation $P_{v_{sat}}(T)$ is given in millibar by the expression :

$$\begin{aligned} log_{10} P_{v_{sat}}(T) = C_0(1 - \frac{T_1}{T}) - C_1 log_{10}\frac{T}{T_1} + \\ C_2(1 - 10^{-C_3(T/T_1 - 1)}) + \\ C_4(10^{C_5(1 - T_1/T)} - 1) + C_6 \end{aligned} \quad (40)$$

The activity $a_w(\bar{\chi})$ is the solution of :

$$\frac{a_w(\bar{\chi})}{\bar{\chi}} = A_1 a_w^2(\bar{\chi}) + A_2 a_w(\bar{\chi}) + A_3 \quad (41)$$

with :

$$A_1 = K_k \frac{\frac{1}{c} - 1}{\chi_m} \quad (42)$$

$$A_2 = \frac{1 - \frac{2}{c}}{\chi_m} \quad (43)$$

$$A_3 = \frac{1}{\chi_m \, c \, K_k} \quad (44)$$

### 6.3 Energical balance

The absorption coefficient $\alpha_{ir}(\bar{\chi})$ is given by :

$$\begin{aligned} \alpha_{ir}(\bar{\chi}) = \alpha_p(\bar{\chi})(1 - \rho_p) + \alpha_s(1 - \rho_p)(1 - \alpha_p(\bar{\chi})) + \\ \alpha_p(\bar{\chi})(1 - \alpha_s)(1 - \rho_p)(1 - \alpha_p(\bar{\chi})) \end{aligned} \quad (45)$$

with :

$$\alpha_p(\bar{\chi}) = 1 - [aa_3(\frac{\bar{\chi}}{\bar{\chi_0}})^3 + aa_2(\frac{\bar{\chi}}{\bar{\chi_0}})^2 + aa_1\frac{\bar{\chi}}{\bar{\chi_0}} + aa_0]\frac{1}{1 - \rho_p} \quad (46)$$

The latent heat coefficient $l_v(T)$ and the calorific thermal capacity $C_p(\bar{\chi}, T)$ are expressed with the temperature in Celsius degrees :

$$l_v(T) = [a_5 T^5 + a_4 T^4 + a_3 T^3 + a_2 T^2 + a_1 T + a_0] * 10^3 \quad (47)$$

$$C_p(\bar{\chi}, T) = [oT + b + \bar{\chi}\{c_{p_3} T^3 + c_{p_2} T^2 + c_{p_1} T + c_{p_0}\}] * 10^3 \quad (48)$$

### 6.4 Numerical values

The numerical values are :

- for the diffusion coefficient $D_{eff}$ :

| Name | Value | Unit |
|---|---|---|
| $D_0$ | $0.68\ 10^{-5}$ | $m^2.s^{-1}$ |
| $a$ | $0.42\ 10^{-1}$ | $kg.kg^{-1}$ |
| $Ea$ | 26464 | $J.mol^{-1}$ |
| $R$ | 8.314 | $J.mol^{-1}.K^{-1}$ |
| $\phi$ | 1.1685 | $m.m^{-1}$ |
| $e_{sec}$ | 102.138 | $\mu m$ |

- for the drying velocity $\dot{m}$ :

| Name | Value | Unit |
|---|---|---|
| $k_m$ | $5.19\ 10^{-3}$ | $m.s^{-1}$ |
| $m_v$ | $18\ 10^{-3}$ | $kg.mol^{-1}$ |
| $T_1$ | 273.16 | $^oK$ |
| $P_t$ | $1.01325\ 10^5$ | $Pa$ |

- to smooth the saturation vapor pressure expression $P_{v_{sat}}$ :

| Name | Value | Unit |
|---|---|---|
| $C_0$ | 10.79574 | (-) |
| $C_1$ | 5.028 | (-) |
| $C_2$ | $1.50475\ 10^{-4}$ | (-) |
| $C_3$ | 8.2969 | (-) |
| $C_4$ | $0.42873\ 10^{-3}$ | (-) |
| $C_5$ | 4.76955 | (-) |
| $C_6$ | 0.78614 | (-) |

- for the activity $a_w$ :

| Name | Value | Unit |
|---|---|---|
| $K_k$ | 0.985 | (-) |
| $c$ | 2.21 | (-) |
| $\chi_m$ | 0.0593 | $kg.kg^{-1}$ |

- for the thermal balance :

| Name | Value | Unit |
|---|---|---|
| $h_c$ | 3 | $W.m^{-2}.K^{-1}$ |
| $\sigma$ | $5.67\ 10^{-8}$ | $W.m^{-2}.K^{-4}$ |
| $\sigma_h$ | $0.96\ \sigma$ | $W.m^{-2}.K^{-4}$ |
| $\rho_p$ | 1165 | $kg.m^{-3}$ |
| $\rho_s C_s e_s$ | 3540.16 | $J.m^{-2}.K^{-1}$ |

- to smooth the expression of the absorption coefficient $\alpha_{ir}$ :

| Name | Value | Unit |
|---|---|---|
| $\alpha_s$ | $0.8$ | $(-)$ |
| $\rho_p$ | $0.12$ | $kg.m^{-3}$ |
| $aa_3$ | $0.3751$ | $(-)$ |
| $aa_2$ | $-0.6545$ | $(-)$ |
| $aa_1$ | $-0.129$ | $(-)$ |
| $aa_0$ | $0.939$ | $(-)$ |

- to smooth the expression of the latent heat coefficient $l_v$ :

| Name | Value | Unit |
|---|---|---|
| $a_5$ | $-0.69851352\ 10^{-9}$ | $kJ.kg^{-1}.^oC^{-5}$ |
| $a_4$ | $0.47175172\ 10^{-6}$ | $kJ.kg^{-1}.^oC^{-4}$ |
| $a_3$ | $-0.12963934\ 10^{-3}$ | $kJ.kg^{-1}.^oC^{-3}$ |
| $a_2$ | $0.12413792\ 10^{-1}$ | $kJ.kg^{-1}.^oC^{-2}$ |
| $a_1$ | $-2.7913724$ | $kJ.kg^{-1}.^oC^{-1}$ |
| $a_0$ | $0.25037\ 10^{4}$ | $kJ.kg^{-1}$ |

- to smooth the expression of the thermal capacity coefficient $C_p$:

| Name | Value | Unit |
|---|---|---|
| $o$ | $0.00647$ | $J.kg^{-1}.K^{-2}$ |
| $b$ | $2.3754$ | $J.kg^{-1}.K^{-1}$ |
| $c_{p_3}$ | $0.749972\ 10^{-7}$ | $J.kg^{-1}.K^{-4}$ |
| $c_{p_2}$ | $-0.943717\ 10^{-5}$ | $J.kg^{-1}.K^{-3}$ |
| $c_{p_1}$ | $0.448761\ 10^{-3}$ | $J.kg^{-1}.K^{-2}$ |
| $c_{p_0}$ | $4.18674$ | $J.kg^{-1}.K^{-1}$ |

## References


[1] Blanc D., Laurent P., Andrieu J., Gerard J.F. *Modeling of the reactive infrared drying of a model water-based epoxy-amine painting coated on iron support with experimental validation*, Proc. 11th *IHTC*, Kyongju, South Korea, Vol. 5, pp. 181–186, 1998.

[2] Dufour P., Touré Y., Laurent P. *A nonlinear distributed parameter process control : an internal linearized model control approach*, Proc. *CESA'98 IEEE IMACS Multiconference*, Hammamet, Tunisia, Vol.1, pp. 134–138, 1998.

[3] Dufour P., Touré Y.,Michaud D.J., Dhurjati P.S. *Optimal trajectory determination and tracking of an autoclave curing process : a model based approach*, Proc. *European Control Conference*, Karslruhe, Germany, Paper No. F1033-6, 1999.

[4] Fletcher R *Practical methods of Optimization*, John Wiley and Sons, 1987.

[5] Ibragimov N.Kh., Shabat A.B. *Evolutionnary equations with nontrivial* L*ie*-B*acklund group*, Functionnal Analysis and the Application, Vol. 14, pp. 19–28, 1980.

[6] Magri F. *Equivalence transformations for nonlinear evolution equations*, J. of Math. Physics, Vol. 18, No. 7, pp. 1405–1411, 1977.

[7] Marquis P., Broustail J.P. SMOC, *a bridge between state space and model predictive controllers : application to the automation of a hydrotreating unit*, Proc. *1988 IFAC Workshop on Model Based Process Control*, pp. 37-43, 1998.

[8] Morari M., Zafiriou E. *Robust control*, Dunod, 1983.

[9] Propoi A.I, *Use of linear programming methods for synthesizing sampled-data automatic systems*, Automn. Remote Control, Vol. 24, No. 7, pp. 837–844, 1963.

[10] Qin S.J., Badgwell T.A., *An overview of industrial model predictive control technology*, Proc. *Fifth International Conference on Chemical Process Control*, pp. 232–256, 1996.

[11] Richalet J., Rault A., Testud J.L., Papon J. *Algorithmic control of industrial processes*, Proc. 4th *IFAC Symposium on Identification and System Parameter Estimation*, Tbilissi, pp. 1119-1167, 1976.

[12] Touré Y., Josserand L. *An extension of IMC to boundary control of distributed parameter systems*, Proc. *IEEE International Conference on Systems, Man and Cybernetics-CCS*, Orlando, USA, Vol. 3, pp. 2426–2431, 1997.